Am. J. Hum. Genet. 73:957–966, 2003

Report

Mutations in Capillary Morphogenesis Gene-2 Result in the Allelic Disorders Juvenile Hyaline Fibromatosis and Infantile Systemic Hyalinosis

Oonagh Dowling,[1] Analisa Difeo,[1] Maria C. Ramirez,[1] Turgut Tukel,[1,6,8] Goutham Narla,[2] Luisa Bonafe,[9] Hulya Kayserili,[7] Memnune Yuksel-Apak,[7] Amy S. Paller,[10] Karen Norton,[3] Ahmad S. Teebi,[11] Valerie Grum-Tokars,[12] Gail S. Martin,[13] George E. Davis,[13] Marc J. Glucksman,[12] and John A. Martignetti[1,4,5]

Departments of [1]Human Genetics, [2]Division of Liver Diseases, [3]Radiology, and [4]Pediatrics and [5]The Derald H. Ruttenberg Cancer Center, Mount Sinai School of Medicine, New York; [6]Istanbul Medical Faculty, Department of Pediatrics, and [7]Child Health Institute, Division of Medical Genetics, and [8]Institute for Experimental Medicine, Department of Genetics, Istanbul University, Istanbul; [9]Division of Molecular Paediatrics, Centre Hospitalier Universitaire Vaudois, Lausanne, Switzerland; [10]Departments of Pediatrics and Dermatology, Children's Memorial Hospital, Northwestern University's Feinberg School of Medicine, Chicago; [11]Department of Genetics, The Hospital for Sick Children, Toronto; [12]Midwest Proteome Center and Department of Biochemistry & Molecular Biology, Finch University of Health Sciences, Chicago Medical School, North Chicago; and [13]Department of Pathology, System Health Science Center, Texas A&M University, College Station

Juvenile hyaline fibromatosis (JHF) and infantile systemic hyalinosis (ISH) are autosomal recessive syndromes of unknown etiology characterized by multiple, recurring subcutaneous tumors, gingival hypertrophy, joint contractures, osteolysis, and osteoporosis. Both are believed to be allelic disorders; ISH is distinguished from JHF by its more severe phenotype, which includes hyaline deposits in multiple organs, recurrent infections, and death within the first 2 years of life. Using the previously reported chromosome 4q21 JHF disease locus as a guide for candidate-gene identification, we identified and characterized JHF and ISH disease-causing mutations in the capillary morphogenesis factor–2 gene (*CMG2*). Although *CMG2* encodes a protein upregulated in endothelial cells during capillary formation and was recently shown to function as an anthrax-toxin receptor, its physiologic role is unclear. Two ISH family-specific truncating mutations, E220X and the 1-bp insertion P357insC that results in translation of an out-of-frame stop codon, were generated by site-directed mutagenesis and were shown to delete the CMG-2 transmembrane and/or cytosolic domains, respectively. An ISH compound mutation, I189T, is predicted to create a novel and destabilizing internal cavity within the protein. The JHF family-specific homoallelic missense mutation G105D destabilizes a von Willebrand factor A extracellular domain alpha-helix, whereas the other mutation, L329R, occurs within the transmembrane domain of the protein. Finally, and possibly providing insight into the pathophysiology of these diseases, analysis of fibroblasts derived from patients with JHF or ISH suggests that *CMG2* mutations abrogate normal cell interactions with the extracellular matrix.

Juvenile hyaline fibromatosis (JHF [MIM 228600]) and infantile systemic hyalinosis (ISH [MIM 236490]) are autosomal recessive disorders that present in infancy with papulonodular skin lesions, particularly of the perianal, perinasal, and perioral areas. Affected individuals often develop several associated features, including multiple subcutaneous tumors, gingival hypertrophy, flexion contractures of joints, osteolytic lesions, and osteopenia (Landing and Nadorra 1986; Fayad et al. 1987; Keser et al. 1999). ISH is distinguished by an earlier onset, more painful and severe course, and, as revealed by histological examination, widespread deposition of hyaline material throughout the skin, gastrointestinal tract, endocrine glands, and muscle (Landing and Nadorra 1986). In addition, ISH has been associated with an increased susceptibility to bone fractures, infections, and death in infancy (Stucki et al. 2001). Diagnosis is generally made on the basis of clinical findings, including distribution

Received July 1, 2003; accepted for publication July 23, 2003; electronically published September 12, 2003.

Address for correspondence and reprints: Dr. John A. Martignetti, Department of Human Genetics, Mount Sinai School of Medicine, Room 14-70B, 1425 Madison Avenue, New York, NY 10029. E-mail: john.martignetti@mssm.edu

0002-9297/2003/7304-0022$15.00

Figure 1 Radiological features of affected individual in family JHF1. *A*, Frontal view of both hands, revealing diffuse osteopenia and narrowing of interarticular spaces. Multiple subluxations and contractures are present. *B*, Lateral view of the knee, revealing marked narrowing of the joint space (*arrow*) and profound osteopenia.

of skin lesions and biopsy results that typically reveal the presence of an abundant extracellular, acidophilic hyaline material. The etiology of these two disorders, suggested elsewhere to be allelic because of their significant phenotypic overlaps (Mancini et al. 1999), is unknown.

By use of a positional-cloning approach, the JHF disease gene was recently localized to chromosome 4q21 (Rahman et al. 2002). The 5.3-cM/6.9-Mb locus is bounded by microsatellite marker D4S2393 centromerically and D4S395 telomerically (Kong et al. 2002; Rahman et al. 2002). In an attempt to further refine the locus and to investigate the possibility that these clinically overlapping autosomal recessive disorders, JHF and ISH, are indeed allelic, we first ascertained four unrelated families with established clinical diagnoses and features consistent with these syndromes (fig. 1; table 1). After obtaining informed consent and institutional review board approval from the corresponding institutions, blood samples were collected from family members, and genomic DNA was isolated. Using a dense set of microsatellite markers spanning the linked region, we haplotyped all available family members to look for regions that were homozygous-by-descent. Haplotype analysis was performed using eight fluorescently labeled microsatellite

Table 1

Comparison of Features of Patients with JHF and ISH

Feature	Findings in Family[a]			
	JHF1	JHF2	ISH1	ISH2[b]
Consanguinity	+	+	+	−
Ethnic origin	Turkish	African American	Turkish	Swiss
Skin:				
Multiple subcutaneous tumors	+	+	−	+
Thickened firm skin	−	−	+	+
Pearly nodules	+	+	−	+
Perianal granulomas	+	−	−	+
Gingiva:				
Gingival hypertrophy	−	+	−	+
Gingival fibromatosis	+	?	−	?
Skeletal findings:				
Joint contractures	+	−	+	+
Restricted movement of joints	+	−	+	+
Painful joints	+	−	+	+
Osteoporosis	+	?	+	+
Osteopenia	+	?	+	+
Growth:				
Failure to thrive	−	−	+	+
Stunted growth	+	−	−	+
Facial features:				
Coarse face	+	+	−	+
Narrow face	−	−	+	+
Large low-set dysplastic ears	−	−	+	+
Miscellaneous:				
Early death	−	−	+	−
Recurrent infections	±	−	+	−
Histology/accumulation of material:				
In skin	−	+	+	+
In articular soft tissues	?	−	?	+

[a] + = feature present; − = feature absent; ± = ambiguous finding; ? = unknown.
[b] Family ISH2 has been described elsewhere (Stucki et al. 2001).

markers (D4S2393, D4S2947, D4S2964, D4S3243, D4S2922, D4S2932, D4S3088, and D4S395). Markers were amplified by PCR with standard protocols, products were run on an ABI 3100 Genetic Analyzer (Applied Biosystems), and electropherograms were analyzed by the ABI Genescan and Genotyper software packages (Perkin Elmer), as we described elsewhere (Heath et al. 2001). Microsatellite order and distances were determined using the Marshfield, UCSC Genome Browser, and Decode databases.

Probands in families ISH1 and JHF2 were homoallelic for all eight markers, which, although consistent with the previous linkage report, did not further narrow the region (fig. 2). Support for the originally defined centromeric border of the JHF locus was provided by members of the remaining two families. The centromeric boundary of the region was confirmed by the nonhomozygosity of marker D4S2393 in the JHF1 affected individual, in whom all other tested markers were homoallelic. It is interesting that, although the affected haplotypes of family ISH2 suggested a potential narrowing of the distal boundary of the region—as demonstrated by homozygosity of three contiguous markers, D4S2947, D4S2964, and D4S3243—we could not rule out the likelihood that this merely reflected "identity-by-state." Therefore, the candidate-gene interval could not be conclusively narrowed. This caution was found to be supported by DNA sequence analysis (see below).

Inspection of genes in the JHF/ISH common region, by use of a combination of public and private databases (e.g., Celera), revealed a number of possible disease-gene candidates, including bone morphogenetic protein 3 (*BMP3*), fibroblast growth factor-5 (*FGF5*), and capillary morphogenesis protein 2 (*CMG2*). Of these, *CMG2* was immediately attractive because of its expression in endothelial cells and its suggested role in binding extracellular matrix (ECM) proteins, including laminin and collagen IV, by virtue of its von Willebrand factor A (VWFA)–like domain (Bell et al. 2001). In addition, the phenotypes of murine knockouts of *BMP3* and *FGF5* genes reported elsewhere were not consistent with either JHF or ISH (Hebert et al. 1994; Daluiski et al. 2001).

Whereas CMG-2 was originally identified on the basis of its up-regulation in endothelial cells induced to undergo

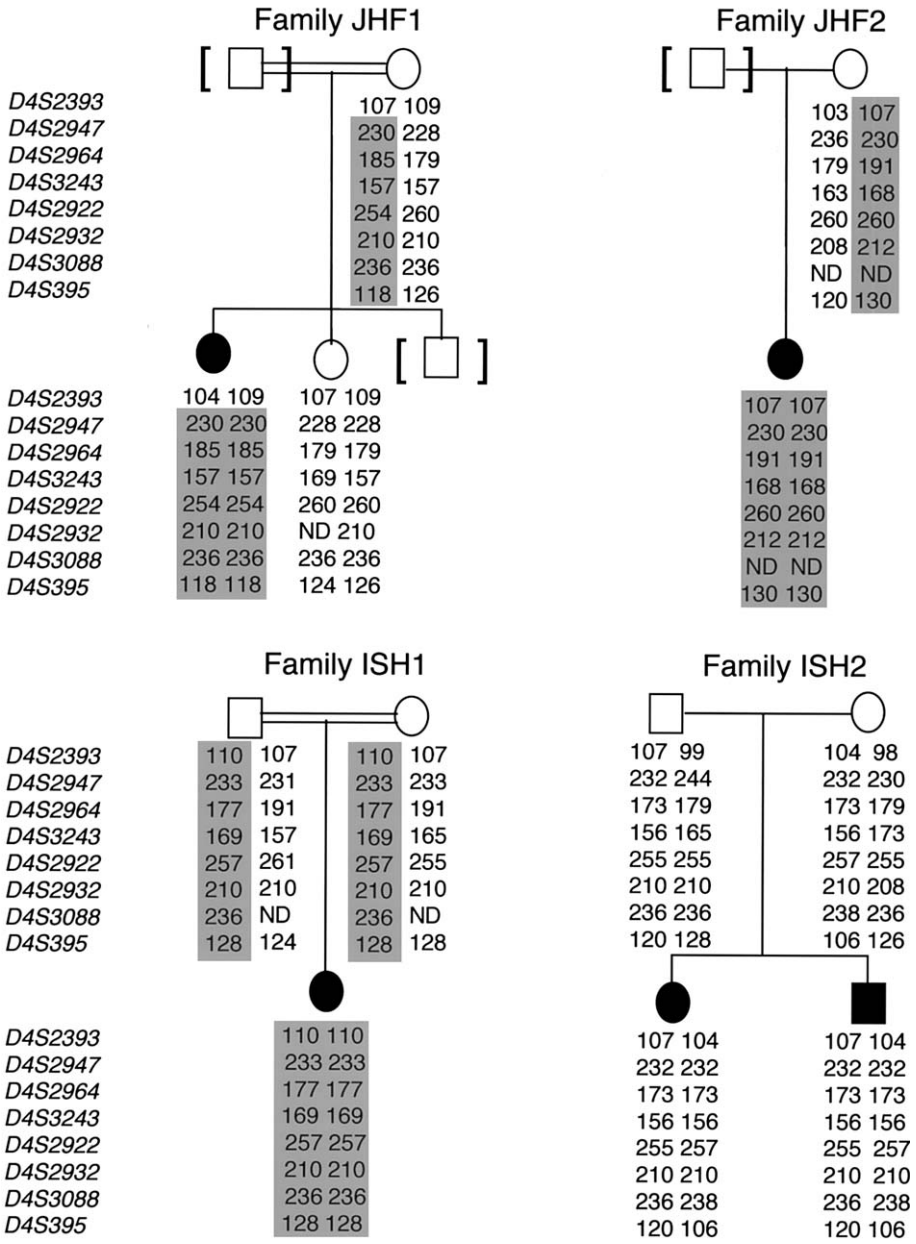

Figure 2 Analysis of pedigrees and haplotypes in four families with JHF or ISH. Genotypes are represented by allele sizes (bp), and markers are shown according to their physical order. Blackened symbols denote affected individuals, and shaded areas denote disease-segregating haplotypes.

capillary formation (Bell et al. 2001), the physiologic role of CMG-2 is unknown. It is interesting that CMG-2 not only possesses protein-sequence similarity to the tumor endothelial marker 8 (*TEM8*) gene—a cell-surface receptor that may play a role in neovascularization and is also the human anthrax-toxin receptor (*ATR*)—but was also recently shown to function as the second known human ATR (Scobie et al. 2003). The predicted topology of CMG-2 is similar to ATR/TEM8 in that they both have a signal peptide, type 1 transmembrane (TM) region, and, within the VWFA or I domain, share 60% identity (fig. 3*A*) (Bell et al. 2001).

We therefore directed our study to determine whether *CMG2* mutations could result in JHF and ISH. We first analyzed all human and nonhuman EST, mRNA data, and gene-prediction output (UCSC Genome Browser [November 2002 and April 2003 assembly dates]) to identify possible coding regions, since several isoforms had been predicted (Scobie et al. 2003). From this combined information, primer pairs were designed to amplify all

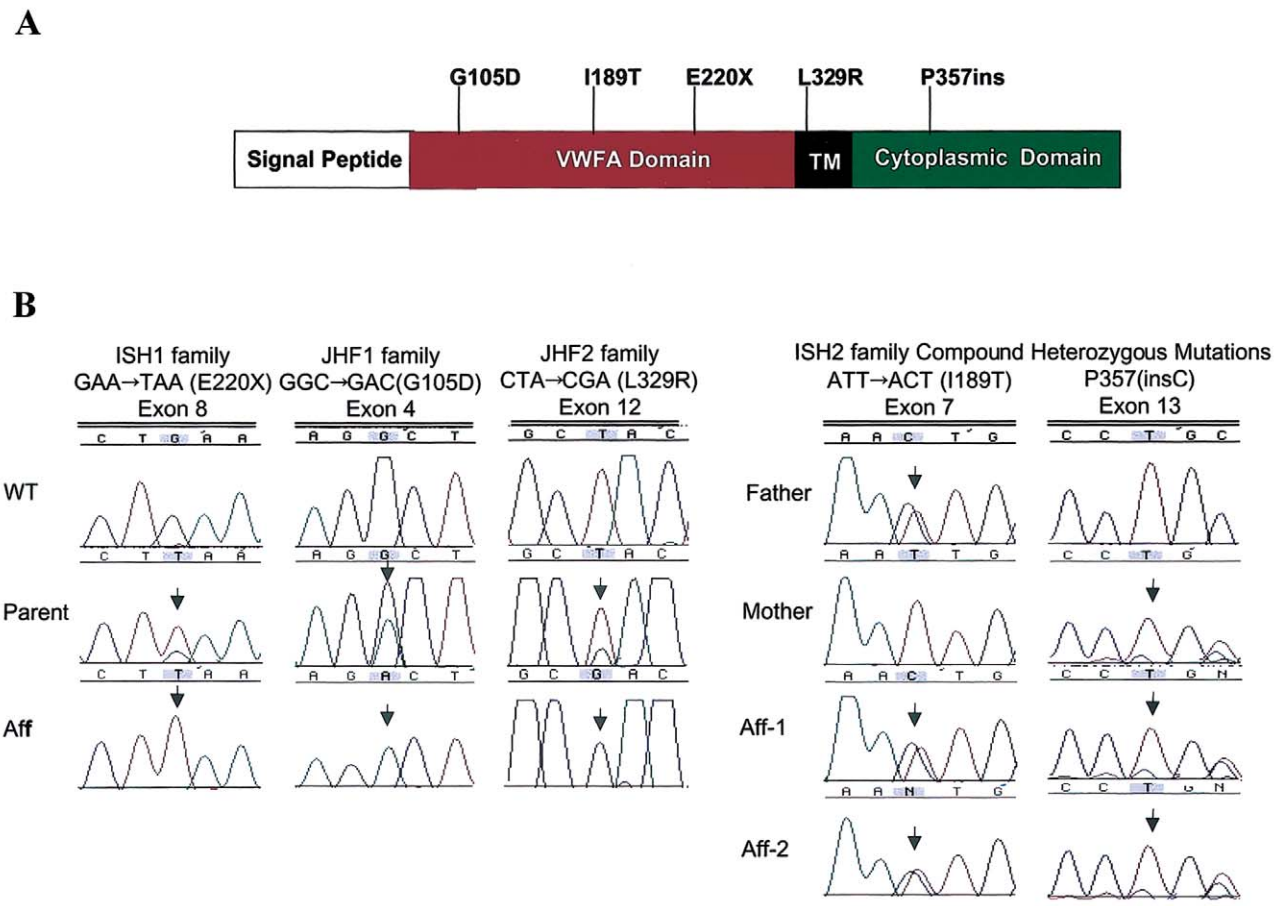

Figure 3 *A*, Predicted CMG-2 protein domains. The protein is 487 amino acids in length and contains an N-terminal signal peptide, followed by a VWFA domain, a TM domain, and a cytosolic tail. Mutations were identified in exons 3, 7, 8, and 12 and are shown relative to affected protein domains. *B*, DNA sequence analysis of CMG-2 in individuals with ISH and JHF. Three homozygous mutations were identified: GAA→TAA (E220X) nonsense mutation in exon 8 of ISH1 family, GGC→GAC (G105D) missense mutation in exon 4 of JHF1 family, and CTA→CGA (L329R) missense mutation in exon 12 of JHF2 family. Both affected children in family ISH2 were compound heterozygotes: ATT→ACT (I189T) missense mutation (paternal allele) and a nucleotide insertion (P357insC) (maternal allele).

17 predicted exons and intron/exon boundaries. Here, we describe the CMG-2-488 isoform that is conserved with the originally cloned CMG-2-386 isoform (Bell et al. 2001) but includes an inserted 100–amino acid membrane-proximal region between the VWFA-like domain and the TM region, as well as 12 alternative amino acids at the C-terminus (fig. 3*A*). PCR products were sequenced in both directions with the ABI BigDye terminator sequencing kit (Perkin Elmer), and data were analyzed using Sequencher 4.1 (GeneCodes). We also explored the possible structure-function effects of patient mutations by first identifying an appropriate model template. On the basis of sequence analysis that demonstrated 48% homology, chain A of the Alpha-X Beta2 Integrin I Domain (Protein Data Bank accession number 1N3Y) was chosen as a template, since the structure was solved by X-ray diffraction to atomic resolution (fig. 4). Nonconserved residues from this domain were mutated *in silico* to the corresponding CMG-2 sequences with the program O (Jones et al. 1991). The CMG-2 model was energy minimized, and the effect of mutations on energy minimization, surface accessibility, interatomic distances, and potential atomic interactions was evaluated using the Molecular Operating Environment suite of programs (Chemical Coupling Group).

CMG2 mutations were identified in all affected individuals, and these mutations were predicted either to truncate or to functionally disrupt the wild-type (WT) protein. None of the mutations identified in any of the families were present in the genomic DNA isolated from 50 unrelated control subjects (100 chromosomes). In family ISH1, the affected individual was found to be homoallelic for a nonsense mutation, a GAA→TAA transversion in codon 220 of exon 8 (E220X) (fig. 3). This mutation

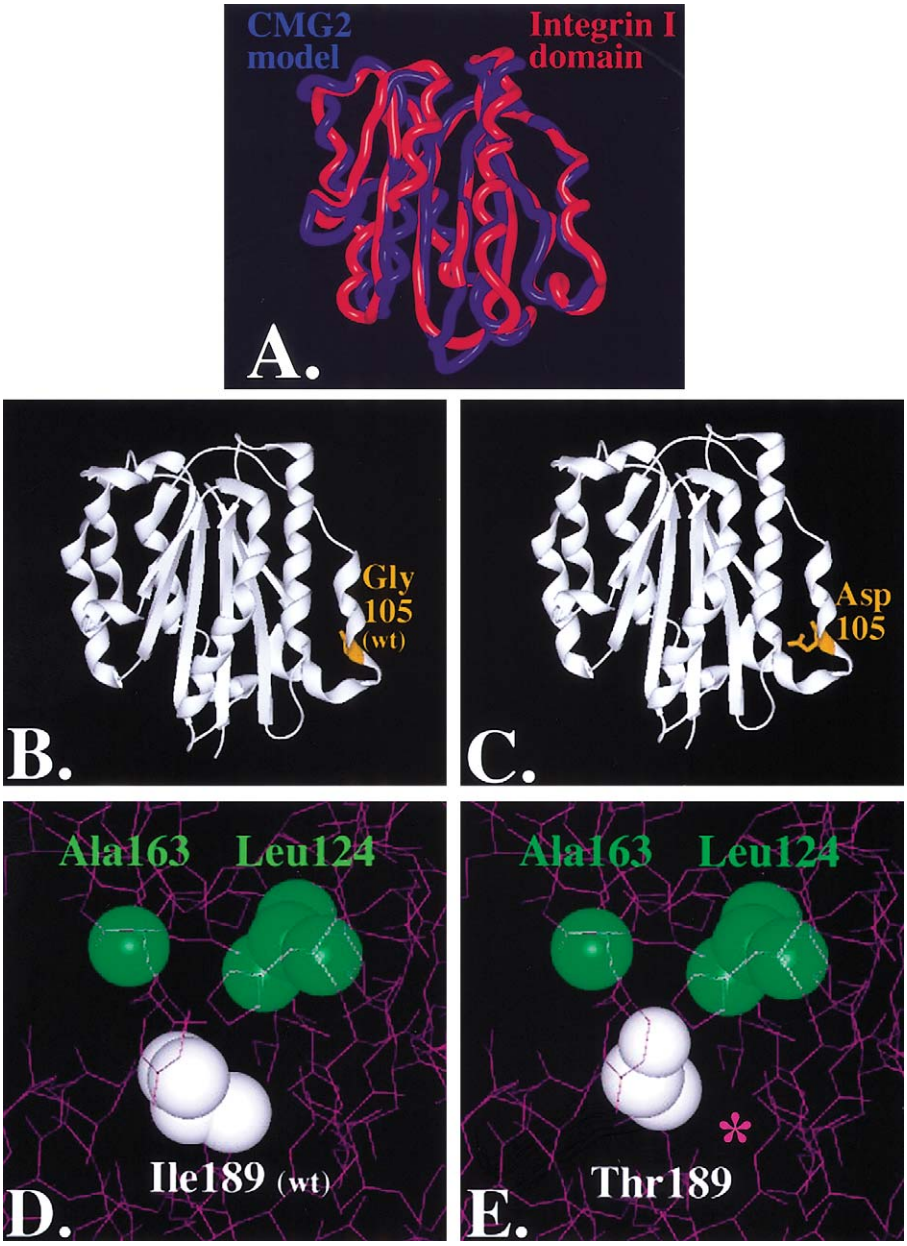

Figure 4 Molecular modeling of CMG-2 mutations: superposition of CMG-2 model (*red*) with chain A of the Alpha-X Beta2 Integrin I Domain (PDB accession number 1N3Y) (*blue*). Nonconserved residues were mutated using the software program O (Jones et al. 1991), and the CMG-2 model was energy minimized using Molecular Operating Environment software (*A*). The root mean square deviation of the CMG-2 model from the integrin template is ~.103 nm, with greater variation in the loops and less variance in the conserved regions where the mutations reside. Glycine 105 (*B*) was mutated to an aspartate (*C*), within the extracellular region and rendered with SPOCK and Raster3D (Merritt and Bacon 1997). Isoleucine 189 (*D*) was mutated to threonine (*E*), and contours were provided by the calculated electron density. A cavity is formed, as indicated by the purple asterisk (*) in panel *E*.

predicts the loss of the majority of the WT proteins, including the TM and cytosolic domains (fig. 3).

DNA sequence analysis of family JHF1 determined the presence of a homozygous change in codon 105 of exon 4, a GGC→GAC transition, which predicted the replacement of a glycine by an aspartate (G105D) in the VWFA-like domain (fig. 3). VWFA domains are found in a number of ECM proteins, including integrins, some collagens, and the matrilins (Hohenester and Engel 2002; Whittaker and Hynes 2002). Indeed, mutations in the VWFA domain of the matrilin-3 protein have been found elsewhere to result in an osteochondrodysplasia, multiple

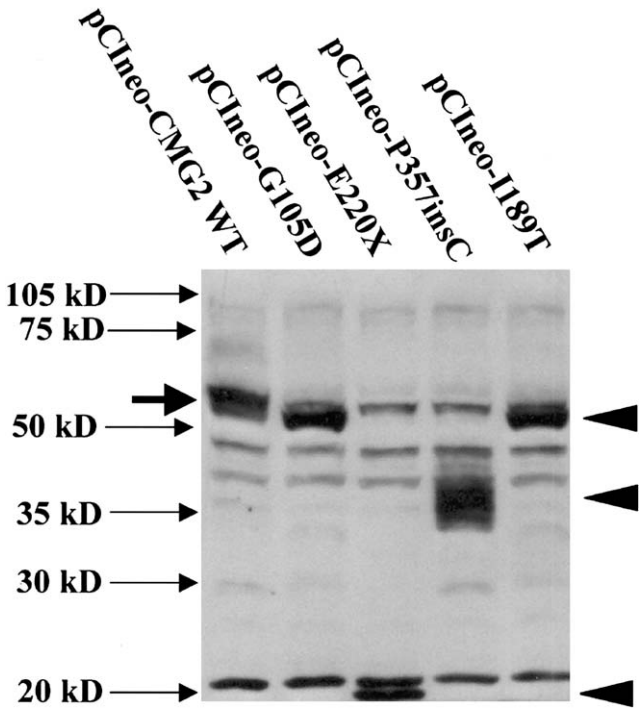

Figure 5 CMG-2 mutations, resulting in altered CMG-2 protein expression, as detected by western blotting. Two hundred ninety-three cells were transfected with 1.5 mg of plasmid DNA (in six-well dishes) with Lipofectamine 2000 and various CMG-2 WT and mutant constructs, as indicated. Following transfection, cells were lysed after 24 h with 0.5 ml SDS-PAGE sample buffer, containing mercaptoethanol, and were treated at 100°C for 10 min. Thirty milliliters of sample was loaded per lane on a 10% SDS-PAGE gel, and protein samples were transferred to PVDF membranes and were probed with anti-CMG-2 affinity-purified antibodies (1 mg/ml), as described elsewhere (Bell et al. 2001). Closed arrowheads indicate the position of anti-CMG-2 reactive mutant proteins. Solid arrow indicates the position of CMG-2 WT protein observed in 293 cells transfected with pCIneo-CMG2-WT.

epiphyseal dysplasia (MIM 607078) (Chapman et al. 2001). Although this domain is involved in ligand recognition in non-ECM molecules, little is known about its role in ECM-molecule function (Hohenester and Engel 2002). Structure alignment of the G105D mutation suggests that the WT glycine residue maps to the carboxy-terminal end of an alpha-helix containing the Schellman motif (fig. 4) (Aurora and Rose 1998). Therefore, the replacement of glycine by aspartate, a nonconserved acidic residue, would be strongly suspected of destabilizing the critical helical "cap" of this secondary structure motif and would argue for the pathogenicity of the mutation.

In family JHF2, we detected a homoallelic mutation in codon 329 of exon 12, a CTA→CGA transversion (fig. 3). It is significant that this is predicted to result in the nonconserved replacement of a leucine residue by an arginine (L329R) within the TM domain (fig. 3). This change from hydrophobic to charged amino acid alters the calculated hydropathy and charge profile of the TM domain. Speculating on the pathophysiologic role of this mutation by analogy with other TM protein regions, the altered CMG-2 leucine is in the center of a stretch of five contiguous leucines within the TM region and thus could effect problems in cell-surface expression, affinity for other TM regions or for ligand binding, and subsequent signaling (Scott et al. 1998). Alternatively, if CMG-2 is in a monomeric state, the introduction of an aspartate may cause receptor aggregation by placing a buried charge within the membrane.

It is surprising that the affected individuals in family ISH2 were found to be compound heterozygotes for CMG-2 disease mutations. In accord with the identified germline mutations, RNA isolated and directly sequenced from cultured fibroblasts confirmed the existence of two transcripts (data not shown). First, each individual possessed a 1-bp C-nucleotide insertion in codon 357 of exon 13, predicting a frameshift mutation, incorporation of a novel 12–amino acid carboxy-tail, and a premature downstream stop codon (TGA; P357insC). The P357insC truncation results in the loss of the terminal 132 amino acid residues that constitutes the cytoplasmic domain (fig. 3). Although no functional roles have yet been defined for this region, it would be expected that this truncated cytoplasmic domain is normally an important modulator in relaying signals across the plasma membrane. In fact, two Wiskott-Aldrich syndrome protein–homology 1 domains are present in this region (Bell et al. 2001), and, therefore, loss of both of these domains could result in loss of actin cytoskeleton interaction.

The second mutation, in codon 189 of exon 7, was predicted to replace an isoleucine with a polar-threonine (I189T) residue (fig. 3). For the I189T mutation, the larger isoleucine-hydrophobic side chain is replaced by a threonine, creating a smaller polar residue toward the interior of the protein. We calculated that the I189T mutation results in the production of an internal 4-nm^3 cavity within the protein (fig. 4*E*), thus completely altering the hydrophobic forces within the protein (Takano et al. 2003). Ultimately, biochemical and structure-function studies will be required to verify these predictions.

To examine the effects of patient-derived mutations on protein synthesis, we generated cDNAs encoding all identified CMG-2 protein mutants by site-directed mutagenesis. The patient mutations were introduced using the Quick-Change site-directed mutagenesis kit, according to the manufacturer's protocol (Stratagene), and all constructs were sequenced in both orientations prior to transfection into 293 cells. Western blots were performed on cell lysates with an affinity–purified rabbit polyclonal antibody directed to the CMG-2 VWFA domain (Bell et al. 2001). As shown in figure 5, all of the patient-derived CMG-2 cDNA constructs are expressed and translated.

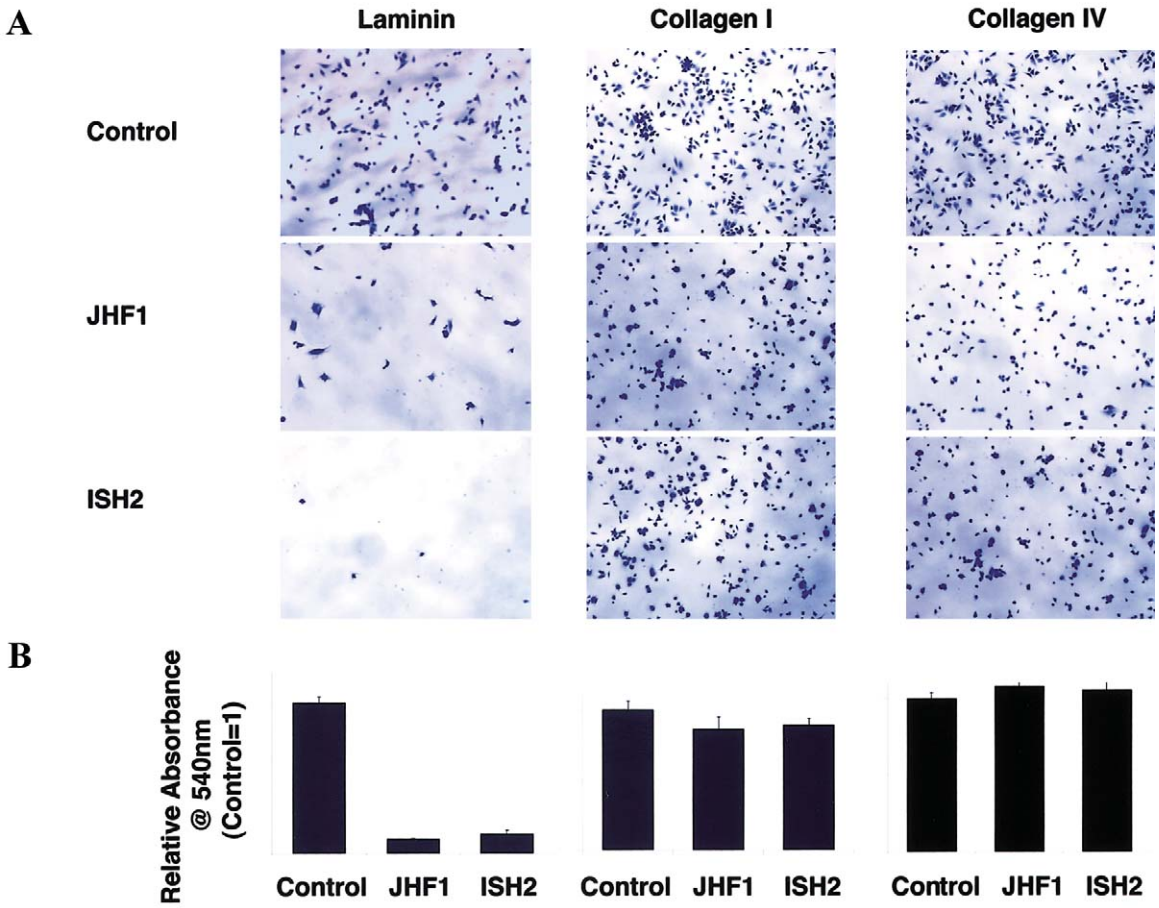

Figure 6 Crystal violet staining of adherent patient and control primary fibroblasts to laminin, collagen I, and collagen IV ECM. Cells were plated in serum-free media at a density of 1×10^5 cells/well and were allowed to adhere to laminin, collagen I, and collagen IV 24-well plates (BD Biosciences) for 75 min. Unbound cells were removed by washing with PBS, and adherent cells were fixed in ethanol (10 min), were stained with 0.5% crystal violet (20 min), were washed extensively with water, and were solubilized with 800 μl 1% SDS. Relative adhesion was quantified by monitoring the absorbance of released dye at 540 nm ($n = 4$). Experiments were repeated three times in quadruplicate. Cells are shown at 7.5× magnification. Bar charts indicate adhesion of patient cells compared with control cells.

It is most notable that, whereas WT CMG-2 protein (pCIneo-CMG2-WT) (fig. 5) migrates at ~55 kDa, the E220X and P357insC mutations resulted in products migrating at ~20 kDa and ~35–40 kDa, respectively. The masses of both of these proteins were consistent with the size of the predicted truncation products. It is interesting that the P357insC-directed protein results in multiple tightly migrating bands, which would suggest either post-translational modification differences—possibly glycosylation—or that the mutated protein is unstable and being degraded.

Functional studies were then performed using patient fibroblasts, the results of which suggested that altered CMG-2/laminin interaction may play a role in disease pathogenesis. The VWFA domain of the CMG-2 protein that is produced as a recombinant protein in bacteria was shown elsewhere to bind both laminin and type IV collagen (Bell et al. 2001). Along with its homology to Alpha-X Beta2 Integrin I Domain, this binding pattern is suggestive of a potential role for CMG-2 in the modulation of cell-matrix or cell-cell interactions, possibly in the capacity of a matrix receptor. Therefore, we examined the ability of fibroblasts of patients with JHF and ISH to attach, spread, and grow on a variety of matrices. Primary dermal fibroblasts from patients JHF1 and ISH2 were plated on laminin, collagen I–, and collagen IV–containing tissue culture plates (BD Biosciences), and the relative adhesion was quantified (Ellerbroek et al. 2001). JHF and ISH fibroblasts were unable to adhere or attach themselves to a laminin matrix (fig. 6), whereas no measurable differences were noted for attachment to collagen types I and IV (fig. 6*A* and 6*B*).

Members of the laminin family of heterotrimeric glycoproteins that contain α, β, and γ chains are major con-

stituents of basement membranes, which are ECMs found in close contact with individual cells and cell layers (Jones et al. 2000). Acting through specific receptors, laminin is crucial for the formation of direct contacts between the ECM and cells. As would be expected, inherited defects in laminins are associated with human disease (McGowan and Marinkovich 2000). For example, epidermolysis bullosa letalis (MIM 226700) is caused by mutations in any of the three laminin-5–associated glycoproteins, $\alpha 3$ (*LAMA3*), $\beta 3$ (*LAMB3*), or $\gamma 2$ (*LAMC2*) (Pulkkinen and Uitto 1999). In addition, and beyond their structural roles, laminins help control cellular activities by allowing the bridging together of information between adjacent cells through interaction with cell surface receptors. It is striking that mutations in the epithelial-expressed, heterodimer-linked laminin-receptor proteins, integrin-$\beta 4$ gene (*ITGB4*), and integrin-$\alpha 6$ gene (*ITGA6*) cause disease in a subset of these patients but with additional gastrointestinal manifestations: epidermolysis bullosa with pyloric atresia (MIM 226730) (Vidal et al. 1995; Ruzzi et al. 1997). Mutations in any component of dystroglycan, a major receptor for $\alpha 2$-laminins in the muscle sarcolemma, result in a range of muscular dystrophies that can be characterized by loss of basement-membrane architecture and function (Colognato and Yurchenco 2000). Also, basement-membrane assembly is thought to be regulated by epithelial-mesenchymal interactions (Lonai 2003), and CMG-2 may play a role in such interactions.

The discovery that *CMG2* mutations result in the allelic disorders JHF and ISH provides a noninvasive molecular diagnostic tool, defines these two diseases as being on either end of the same disease spectrum, and highlights novel information on the in vivo function of this integrin-like cell surface molecule and its role in key developmental and physiological processes. The dermal, gastrointestinal, and skeletal findings present in these syndromes could result from dysregulation in basement-membrane architecture, possibly arising from compromised cell-matrix or cell-cell interactions. Histologic reports have identified cells embedded within a fibrillogranular material with cellularity inversely proportional to the age of the lesion and with abnormal accumulation of extracellular deposits that apparently originate from dermal blood vessels (Stucki et al. 2001). This strengthens the hypothesis that CMG-2 plays a role in basement membrane–matrix homeostasis and architecture during development and morphogenesis (Bell et al. 2001) and provides the starting point for future studies.

Acknowledgments

We thank the families and referring physicians, especially Dr. Judith Dillner (Mount Sinai School of Medicine), for their participation in this study, and Abigail Guce and Vanessa Mendoza (Mount Sinai School of Medicine), for their expert technical assistance. This work was supported, in part, by National Institutes of Health National Center for Research Resources grant S10 RR 015935 (to M.J.G.) and National Heart, Lung, and Blood Institute grant HL59373 (to G.E.D).

Electronic-Database Information

URLs for data presented herein are as follows:

Celera, http://www.celera.com/ (for identification of candidate genes)
Center for Medical Genetics, Marshfield Medical Research Foundation, http://research.marshfieldclinic.org/genetics/
Decode, http://www.decodegenetics.com/ (for the human genetic map)
Online Mendelian Inheritance in Man (OMIM), http://www.ncbi.nlm.nih.gov/Omim/ (for JHF, ISH, epidermolysis bullosa letalis, epidermolysis bullosa with pyloric atresia, and multiple epiphyseal dysplasia)
Protein Data Bank, http://www.rcsb.org/pdb/
UCSC Genomic Bioinformatics, http://genome.cse.ucsc.edu/

References

Aurora R, Rose GD (1998) Helix capping. Protein Sci 7:21–38
Bell SE, Mavila A, Salazar R, Bayless KJ, Kanagala S, Maxwell SA, Davis GE (2001) Differential gene expression during capillary morphogenesis in 3D collagen matrices: regulated expression of genes involved in basement membrane matrix assembly, cell cycle progression, cellular differentiation and G-protein signaling. J Cell Sci 114:2755–2773
Chapman KL, Mortier GR, Chapman K, Loughlin J, Grant ME, Briggs MD (2001) Mutations in the region encoding the von Willebrand factor A domain of matrilin-3 are associated with multiple epiphyseal dysplasia. Nat Genet 28:393–396
Colognato H, Yurchenco PD (2000) Form and function: the laminin family of heterotrimers. Dev Dyn 218:213–234
Daluiski A, Engstrand T, Bahamonde ME, Gamer LW, Agius E, Stevenson SL, Cox K, Rosen V, Lyons KM (2001) Bone morphogenetic protein-3 is a negative regulator of bone density. Nat Genet 27:84–88
Ellerbroek SM, Wu YI, Overall CM, Stack MS (2001) Functional interplay between type I collagen and cell surface matrix metalloproteinase activity. J Biol Chem 276:24833–24842
Fayad MN, Yacoub A, Salman S, Khudr A, Der Kaloustian VM (1987) Juvenile hyaline fibromatosis: two new patients and review of the literature. Am J Med Genet 26:123–131
Heath KE, Campos-Barros A, Toren A, Rozenfeld-Granot G, Carlsson LE, Savige J, Denison JC, Gregory, MC, White JG, Barker DF, Greinacher A, Epstein CJ, Glucksman MJ, Martignetti JA (2001) Nonmuscle myosin heavy chain IIA mutations define a spectrum of autosomal dominant macrothrombocytopenias: May-Hegglin anomaly and Fechtner, Sebastian, Epstein, and Alport-like syndromes. Am J Hum Genet 69:1033–1045
Hebert JM, Rosenquist T, Gotz J, Martin GR (1994) FGF5 as a regulator of the hair growth cycle: evidence from targeted and spontaneous mutations. Cell 78:1017–1025
Hohenester E, Engel J (2002) Domain structure and organisation in extracellular matrix proteins. Matrix Biol 21:115–128

Jones JC, Dehart GW, Gonzales M, Goldfinger LE (2000) Laminins: an overview. Microsc Res Tech 51:211–213

Jones TA, Zou JY, Cowan SW, Kjeldgaard A (1991) Improved methods for building protein models in electron density maps and the location of errors in these models. Acta Crystallogr A 47:110–119

Keser G, Karabulut B, Oksel F, Calli C, Ustun EE, Akalin T, Kocanaogullari H, Gumudis G, Doganavsargil E (1999) Two siblings with juvenile hyaline fibromatosis: case reports and review of the literature. Clin Rheumatol 18:248–252

Kong A, Gudbjartsson DF, Sainz J, Jonsdottir GM, Gudjonsson SA, Richardsson B, Sigurdardottir S, Barnard J, Hallbeck B, Masson G, Shlien A, Palsson ST, Frigge ML, Thorgeirsson TE, Gulcher JR, Stefansson K (2002) A high-resolution recombination map of the human genome. Nat Genet 31:241–247

Landing BH, Nadorra R (1986) Infantile systemic hyalinosis: report of four cases of a disease, fatal in infancy, apparently different from juvenile systemic hyalinosis. Pediatr Pathol 6: 55–79

Lonai P (2003) Epithelial mesenchymal interactions, the ECM and limb development. J Anat 202:43–50

Mancini GM, Stojanov L, Willemsen R, Kleijer WJ, Huijmans JG, van Diggelen OP, de Klerk JB, Vuzevski VD, Oranje AP (1999) Juvenile hyaline fibromatosis: clinical heterogeneity in three patients. Dermatology 198:18–25

McGowan KA, Marinkovich MP (2000) Laminins and human disease. Microsc Res Tech 51:262–279

Merritt EA, Bacon DJ (1997) Raster3D: photorealistic molecular graphics. Methods Enzymol 277:505–524

Pulkkinen L, Uitto J (1999) Mutation analysis and molecular genetics of epidermolysis bullosa. Matrix Biol 18:29–42

Rahman N, Dunstan M, Teare MD, Hanks S, Edkins SJ, Hughes J, Bignell GR, Mancini G, Kleijer W, Campbell M, Keser G, Black C, Williams N, Arbour L, Warman M, Superti-Furga A, Futreal, PA, Pope FM (2002) The gene for juvenile hyaline fibromatosis maps to chromosome 4q21. Am J Hum Genet 71:975–980

Ruzzi L, Gagnoux-Palacios L, Pinola M, Belli S, Meneguzzi G, D'Alessio M, Zambruno G (1997) A homozygous mutation in the integrin alpha6 gene in junctional epidermolysis bullosa with pyloric atresia. J Clin Invest 99:2826–2831

Scobie HM, Rainey GJ, Bradley KA, Young JA (2003) Human capillary morphogenesis protein 2 functions as an anthrax toxin receptor. Proc Natl Acad Sci USA 100:5170–5174

Scott JP 3rd, Scott JP 2nd, Chao YL, Newman PJ, Ward CM (1998) A frameshift mutation at Gly975 in the transmembrane domain of GPIIb prevents GPIIb-IIIa expression—analysis of two novel mutations in a kindred with type I glanzmann thrombasthenia. Thromb Haemost 80:546–550

Stucki U, Spycher MA, Eich G, Rossi A, Sacher P, Steinmann B, Superti-Furga A (2001) Infantile systemic hyalinosis in siblings: clinical report, biochemical and ultrastructural findings, and review of the literature. Am J Med Genet 100:122–129

Takano K, Yamagata Y, Yutani K (2003) Buried water molecules contribute to the conformational stability of a protein. Protein Eng 16:5–9

Vidal F, Aberdam D, Miquel C, Christiano AM, Pulkkinen L, Uitto J, Ortonne JP, Meneguzzi G (1995) Integrin beta 4 mutations associated with junctional epidermolysis bullosa with pyloric atresia. Nat Genet 10:229–234

Whittaker CA, Hynes RO (2002) Distribution and evolution of von Willebrand/integrin a domains: widely dispersed domains with roles in cell adhesion and elsewhere. Mol Biol Cell 13:3369–3387